INSTITUTE OF PHYSICS PUBLISHING JOURNAL OF PHYSICS B: ATOMIC, MOLECULAR AND OPTICAL PHYSICS

J. Phys. B: At. Mol. Opt. Phys. **38** (2005) 1329–1340 doi:10.1088/0953-4075/38/8/019

Electron scattering by ytterbium: I. Excitation of the $4f^{14}6s6p\ ^1P_1$ resonance state and elastic collision

B Predojević[1,2], D Šević[1], V Pejčev[1,3], B P Marinković[1] and D M Filipović[1,4]

[1] Institute of Physics, PO Box 68, 11080, Belgrade, Serbia and Montenegro
[2] Faculty of Natural Sciences, University of Banja Luka, Republic of Srpska, Bosnia and Herzegovina
[3] Faculty of Natural Sciences, University of Kragujevac, 34000 Kragujevac, Serbia and Montenegro
[4] Faculty of Physics, University of Belgrade, PO Box 368, 11001, Belgrade, Serbia and Montenegro

E-mail: bratislav.marinkovic@phy.bg.ac.yu

Received 22 November 2004
Published 8 April 2005
Online at stacks.iop.org/JPhysB/38/1329

Abstract

Differential cross sections (DCSs) for electron-impact excitation of the $4f^{14}6s6p\ ^1P_1$ resonance state of ytterbium were measured at 10, 20, 40, 60 and 80 eV incident electron energies (E_0) and scattering angles (θ) between 2° and 150°. The absolute DCS scale for the $^1P_1$ state was determined through normalization of its relative DCSs to the optical oscillator strength using the forward scattering function method. DCSs for elastic electron scattering by ytterbium were measured at the same energies for θ between 10° and 150°. Elastic-to-inelastic intensity ratios were obtained from energy-loss spectra recorded with overall energy resolution of 65 meV (FWHM) and angular resolution of 1.5°. Both inelastic and elastic DCSs were extrapolated to 0° and 180° and numerically integrated to yield integral, momentum transfer and viscosity cross sections. Our results are compared with scarce experimental and theoretical data.

1. Introduction

The ytterbium rare-earth atom has a closed-shell, two (6s) valence electron ground state configuration [Kr] $4f^{14}6s^2\ ^1S_0$. Atoms of the II group, investigated in our previous works (Ca (Milisavljević *et al* 2004), Zn (Predojević *et al* 2003, Panajotović *et al* 2004), Cd (Marinković *et al* 1991) and Hg (Panajotović *et al* 1993)) have the same outer-shell structure. The electronic structure of ytterbium makes this atom very interesting for investigation of a number of electron atom collision processes.

Features in ytterbium spectra give the 'simple' part that corresponds to excitation of the 6s valence electrons in addition to the 'complex' due to excitation of one of the $4f^{14}$ electrons. This heavy atom ($Z = 70$) provides an important test for relativistic effects in electron atom scattering. On the other hand, studies of electron impact by ytterbium are important because of the potential suitability of ytterbium vapour as a laser medium (Cahuzac 1968, Klimkin 1975). Recently, Takasu *et al* (2003) have observed Bose–Einstein condensation in a gas of ytterbium atoms. They also noted that optically trapped Yb atoms have important application in fundamental physics as the test of time-reversal symmetry and parity violation.

Only a very limited number of experimental and theoretical data related to electron scattering by ytterbium is available. An electron energy-loss spectrum of ytterbium was reported initially by Kazakov and Hristoforov (1983) at incident electron energy of $E_0 =$ 14 eV, using a 127° analyser positioned at scattering angle $\theta = 90°$ in the scattering plane perpendicular to the Yb-vapour beam. In the same work they studied resonances in elastic scattering and also the $4f^{14}6s6p\ {}^1P_1$ and $4f^{14}6s6p\ {}^3P_{0,1,2}$ excitation functions. Mandy *et al* (1993) recorded energy-loss spectra at $E_0 = 3.2$, 5.2 and 7.2 eV, and the threshold excitation spectrum at E_0 from 1 to 7 eV.

Optical excitation functions for 36 atomic transitions in Yb and Yb^+, at E_0 from the excitation thresholds to 300 eV, were measured by Shimon *et al* (1981). Johnson *et al* (1998) measured differential cross sections (DCSs) for electron-impact excitation of the $4f^{14}6s6p\ {}^1P_1$ state at $E_0 = 5$, 10, 20, 40 and 80 eV and θ from 2° to 65°. Transition to the absolute DCS scale has been performed by normalization to their theoretical integral cross section at 80 eV, with extrapolation to lower energies based on the shape of the excitation function measured by Shimon *et al* (1981).

The calculations available in the literature are based on the distorted-wave approximation and the phenomenological complex optical potential (OP). Srivastava *et al* (1995) calculated DCSs for the $4f^{14}6s6p\ {}^1P_1$ and $4f^{14}6s6p\ {}^3P_{0,1,2}$ fine-structure levels at $E_0 = 20$ and 40 eV using the relativistic distorted-wave (RDW) approximation. Johnson *et al* (1998) performed the unitarized distorted-wave (UDW) approximation to calculate DCSs for the $4f^{14}6s6p\ {}^1P_1$ level at $E_0 = 5$, 10, 20, 40 and 80 eV. Kelemen *et al* (1995) investigated the elastic and inelastic electron scattering in the energy range $\leqslant$200 eV taking into account the dipole polarizability in the OP model.

In this paper, atomic levels of Yb are identified according to the NIST Atomic Spectra Database (1999). The paper is organized as follows. In section 2, we report improvements of the apparatus, relevant to the Yb target and the experimental procedure. In section 3, a representative electron energy-loss (0 to 6.5 eV) Yb spectrum at $E_0 = 20$ eV ($\theta = 6°$) is shown. Also, results of normalized DCSs for the $4f^{14}6s6p\ {}^1P_1$ level at $E_0 = 10$ to 80 eV (θ from 2° to 150°) and elastic scattering at the same energies and θ from 10° to 150°, together with corresponding integrated—integral (Q_I), momentum transfer (Q_M) and viscosity (Q_V)—cross sections are presented in figures and tables. Finally, discussion and concluding remarks are given in section 4. The other DCSs, for electron-impact excitation of the $4f^{14}6s6p\ {}^3P_1$, $4f^{14}5d6s\ {}^1D_2$, $4f^{13}5d6s^2\ (7/2,5/2)_1$ and $4f^{14}6s7p\ {}^1P_1$ states are reported and discussed in our next paper referred to as II.

2. The experiment and procedure

The apparatus used for the measurements is a conventional cross-beam electron spectrometer described elsewhere (Predojević *et al* 2003). Electron optics of both the monochromator

and the analyser are very similar to that designed by Chutjian (1979). The analyser can be positioned from -30° up to 150° with respect to the mechanical zero. A channel electron multiplier is used for single-electron counting. The spectrometer operates in the energy-loss mode. For each separate experiment, angular distribution of the scattered electron intensity, symmetric around the real zero, has been measured from -20° to $+20^\circ$. In this way, the zero scattering angle was determined with uncertainty of 0.5°. Overall system energy resolution (as FWHM) was about 65 meV in these measurements. The angular resolution of the spectrometer is estimated to be 1.5°. The energy scale was calibrated against the structure at 4.03 eV attributed to the 4 ^{3}P excitation threshold of Zn (Predojević *et al* 2003) measured previously. A pessimistic uncertainty of the energy scale was estimated to be 0.01 (as for Zn) because adhesion of ytterbium (work function $A = 2.59$ eV) within the interaction chamber reduces the work function of its 'Zn-plated' ($A = 4.33$ eV) wall to a value close to that of the thoriated tungsten filament ($A = 2.63$ eV). Setting of the energy is determined by the negative potential of the filament with respect to the grounded interaction chamber. Under these circumstances the potential difference between the filament and the interaction volume, as it is seen by the incident electrons, is less than 2% so one can expect a lower zero shift than in the case of Zn.

The metal-vapour beam source consists of a stainless-steel crucible. The crucible is placed in a stainless-steel cylinder co-axially wrapped with two different resistive bifilar heaters (top and bottom, monitored with two thermocouples), enabling the top of the source to be at approximately 100 K higher than the bottom. This prevents clogging and minimizes dimmer production. An additional outer copper cylinder served as a holder for the helical tube of the water-cooler. This cooler protects the channel electron multiplier during long term measurements. The measurements were performed at a temperature of about 870 K for ytterbium of 99.99% purity. This temperature corresponds to a metal-vapour pressure of about 5.2 Pa, at which ytterbium effused through the cylindrical channel (aspect ratio $\gamma = 0.075$) in the cap of the crucible.

In this work, relative DCSs for both electron-impact excitation of the $4f^{14}6s6p\ ^1P_1$ state and elastic scattering are obtained as follows. At a certain incident electron energy and energy loss (ΔE), the position of the analyser was changed from 2° (10° for elastic) to $+150^\circ$ and the angular distribution of scattered electrons was measured. A correction of the scattering intensity was made due to the angular dependence of the effective interaction volume. The effective path-length correction factors (F) (Brinkman and Trajmar 1981) were calculated using the procedure described by Marinković *et al* (1991) for the Cd atom.

Absolute DCS values for the $4f^{14}6s6p\ ^1P_1$ level are determined through normalization of the relative values utilizing the forward scattering function (FSF) method introduced by Avdonina *et al* (1997). The energy $E_0 = 10$ eV satisfies the statement that the FSF method is applicable from the value $E_0 > 2.5\omega$, where ω is the excitation energy. Optical oscillator strength (OOS) obtained by Komarovskii (1991) was adopted as the generalized oscillator strength (GOS) limit as the squared momentum transfer tends to zero. The absolute elastic DCSs were obtained using absolute DCS values of the $4f^{14}6s6p\ ^1P_1$ state and separately measured elastic-to-inelastic (the resonance $4f^{14}6s6p\ ^1P_1$) intensity ratios. To solve the transmission problem we have measured the intensity ratios of elastic and $4f^{14}6s6p\ ^1P_1$ signals with two different tunings of the analyser. We tuned the analyser to optimize the signal of elastically scattered electrons, and then the signal of scattered electrons after excitation of the $4f^{14}6s6p\ ^1P_1$ state. If only a change of the central potential of the zoom lens at the analyser entrance (3 to 3.5 V) causes changes in the elastic-to-inelastic ratios, and the transmission response has symmetrical behaviour, we assume the true elastic-to-inelastic intensity ratio is the geometrical mean of the values obtained in the two focusing conditions mentioned above.

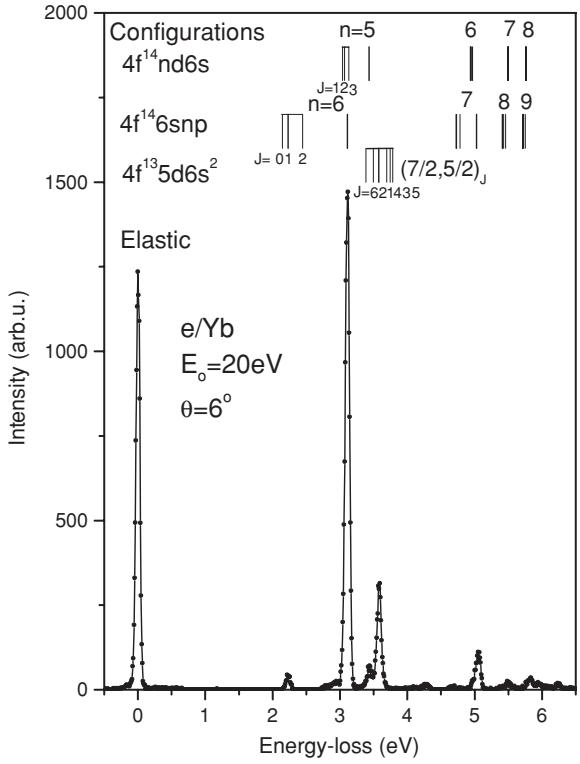

Figure 1. Electron energy-loss spectrum of Yb atom at $E_0 = 20$ eV incident electron energy and $\theta = 6^\circ$ scattering angle.

Both inelastic and elastic DCSs were extrapolated to 0° and 180° and numerically integrated to yield integrated (Q_{I}, Q_{M} and Q_{V}) cross sections.

3. Results

3.1. The $4f^{14}6s6p\ ^1P_1$ resonance state

The energy-loss spectrum at 20 eV impact energy and scattering angle of 6° is shown in figure 1. The $4f^{14}6s6p\ ^1P_1$ feature is positioned at $\Delta E = 3.108$ eV and its peak at 6° is higher than the elastic peak. Below the $4f^{14}6s7p\ ^1P_1$ state positioned at 5.029 eV, features corresponding to the $4f^{14}6s6p\ ^3P_1$, $4f^{14}5d6s\ ^1D_2$ and $4f^{13}5d6s^2\ (7/2,5/2)_1$ states are clearly resolved, except the $4f^{14}5d6s\ ^3D_{1,2,3}$ states which contribute to the $4f^{14}6s6p\ ^1P_1$ prominent feature. One cannot suspect that the contribution of the $4f^{14}5d6s\ ^3D_{1,2,3}$ states is significant in this 'optical like' (high energy, low angle) energy-loss spectrum.

We have measured DCSs for electron-impact excitation of the $4f^{14}6s6p\ ^1P_1$ resonance state at $E_0 = 10$, 20, 40, 60 and 80 eV and θ from 2° to 150°. In a separate series of experiments, relative DCS measurements were performed at numbered impact energies and $\theta \leqslant 10^\circ$ in steps of 2°. From these measurements the relative generalized oscillator strengths were obtained. The FSF with OOS of 1.3 for the $4f^{14}6s6p\ ^1P_1$ state adopted from Komarovskii (1991) is drawn in figure 2. A normalized GOS has been achieved through displacement of our relative GOS at $\theta = 0^\circ$ until its value attained that of the FSF at the corresponding K^2. The GOS values and

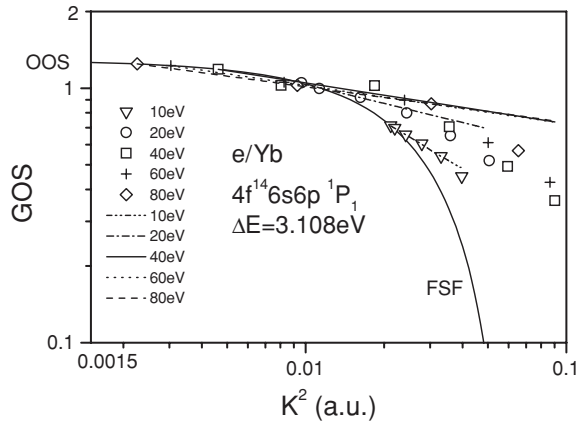

Figure 2. Generalized oscillator strengths for electron-impact excitation of the $4f^{14}6s6p\ ^1P_1$ state of the Yb atom (energy-loss $\Delta E = 3.108$ eV) at 10, 20, 40, 60 and 80 eV incident electron energies.

Table 1. Differential cross sections for electron-impact excitation of the $4f^{14}6s6p\ ^1P_1$ state of ytterbium. The last three rows are integrated—integral (Q_I), momentum transfer (Q_M) and viscosity (Q_V)—cross sections in units of 10^{-20} m^2. The absolute errors are indicated in parentheses.

Scattering angle (°)	DCS (x10^{-20} m^2 sr^{-1})				
	10 eV	20 eV	40 eV	60 eV	80 eV
2	129(16)	398(48)	599(72)	606(73)	557(67)
4	110(14)	255(31)	262(31)	178(21)	144(17)
6	88(11)	147(18)	93.4(11.2)	58.3(7.1)	43.7(5.3)
8	66.0(8.2)	81.5(9.8)	38.9(4.7)	23.4(2.9)	15.0(1.9)
10	46.0(5.5)	46.1(5.6)	18.8(2.3)	9.85(1.20)	5.80(0.72)
20	7.46(0.90)	2.59(0.31)	0.844(0.101)	0.604(0.076)	0.427(0.052)
30	1.19(0.14)	0.445(0.055)	0.257(0.031)	0.218(0.029)	0.126(0.016)
40	0.300(0.037)	0.230(0.029)	0.0811(0.0101)	0.0655(0.0103)	0.0261(0.0039)
50	0.190(0.024)	0.139(0.018)	0.0714(0.0089)	0.0265(0.0053)	0.0073(0.0015)
60	0.140(0.018)	0.0873(0.0115)	0.0255(0.0033)	0.0078(0.0024)	0.0048(0.0011)
70	0.0837(0.0112)	0.0509(0.0070)	0.0093(0.0014)	0.0032(0.0015)	0.0031(0.0009)
80	0.0537(0.0075)	0.0186(0.0032)	0.0070(0.0011)	0.0067(0.0023)	0.0031(0.0009)
90	0.0481(0.0069)	0.0169(0.0031)	0.0158(0.0022)	0.0100(0.0028)	0.0047(0.0012)
100	0.0537(0.0075)	0.0241(0.0037)	0.0236(0.0032)	0.0117(0.0031)	0.0044(0.0011)
110	0.0799(0.0107)	0.0322(0.0045)	0.0235(0.0032)	0.0126(0.0033)	0.0046(0.0011)
120	0.0684(0.0093)	0.0286(0.0041)	0.0141(0.0020)	0.0059(0.0021)	0.0040(0.0010)
130	0.0780(0.0105)	0.0276(0.0040)	0.0079(0.0015)	0.0014(0.0009)	0.0033(0.0009)
140	0.123(0.016)	0.0390(0.0058)	0.0042(0.0008)	0.0017(0.0011)	0.0031(0.0009)
150	0.211(0.027)	0.0971(0.0126)	0.0057(0.0011)	0.0021(0.0012)	0.0049(0.0012)
Q_I	17.2(2.9)	19.4(2.9)	14.8(2.3)	11.6(1.8)	9.76(1.76)
Q_M	4.60(0.76)	2.58(0.40)	0.91(0.14)	0.47(0.08)	0.30(0.06)
Q_V	6.4(1.1)	3.79(0.57)	1.56(0.24)	0.82(0.14)	0.51(0.10)

their linear parts are presented in the same figure by discrete data points and lines, respectively. Finally, the normalized-to-relative GOS quotients have been used as the normalization factors for putting our relative DCSs to the absolute scale.

Absolute DCS values for the $4f^{14}6s6p\ ^1P_1$ state (with absolute errors in parentheses) are given in table 1. These DCSs, with corresponding statistical error bars indicated, are presented

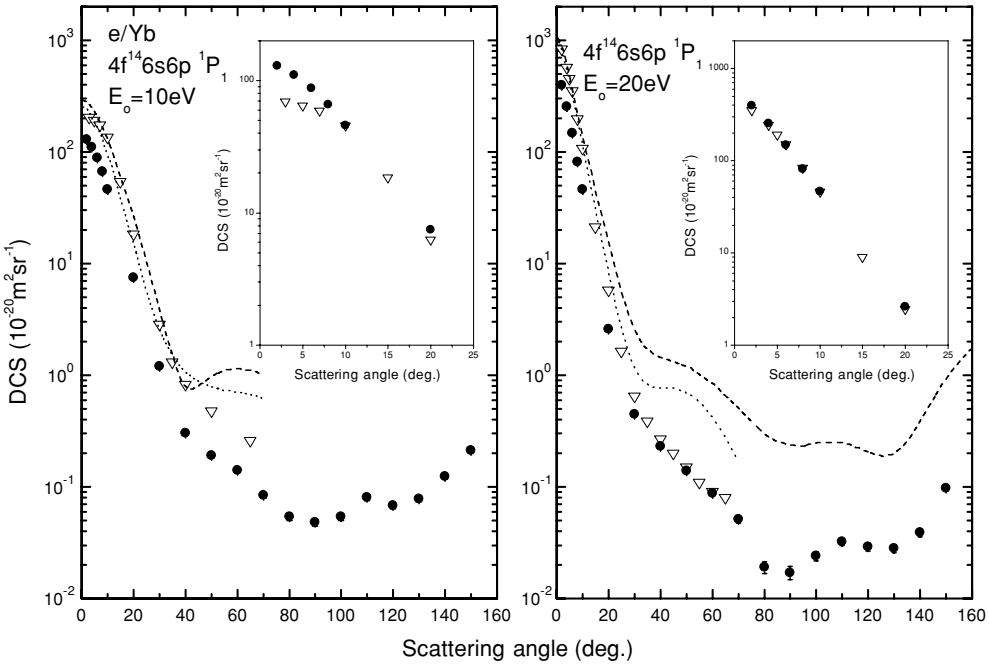

Figure 3. Differential cross sections for excitation of the $4f^{14}6s6p\ ^1P_1$ state at 10 and 20 eV impact energies. Experiments: ●, present (statistical error bars are indicated); ▽, Johnson *et al* (1998). Calculations: ·····, UDW, Johnson *et al* (1998); – – –, RDW, Srivastava *et al* (1995).

in figures 3, 4 and 5. The errors arise from two sources: (a) uncertainties in our experimental values, (b) uncertainty in the normalization procedure. Uncertainties in our experimental values reflect the uncertainty of relative DCSs. This arises from the statistical errors, and uncertainty of θ (0.03), E_0 (0.01) and F (0.06). Uncertainty in the normalization arises from uncertainty of the OOS (0.1) according to Komarkovskii (1991). Total errors of DCSs are obtained as the square root of the sum of squared particular errors.

Integrated (Q_I, Q_M, Q_V) cross sections are obtained by polynomial extrapolation of the absolute DCSs to $\theta = 0^\circ$ and 180°, and numerical integration. Their total absolute errors arise from the DCS errors mentioned above, and extrapolation of DCSs to $\theta = 0^\circ$ and 180° and numerical integration (0.1). Q_I, Q_M and Q_V are given at the bottom in table 1 (with the errors in parentheses), and Q_I is presented in figure 6. In the same figure, both the UDW and RDW theoretical results together with those obtained by Shimon *et al* (1981) (original, and normalized to the present value at 20 eV) are added for comparison.

3.2. The elastic scattering

The relative DCSs for elastic electron scattering were measured at $E_0 = 10$, 20, 40, 60 and 80 eV and θ from 10° to 150°. The absolute DCS values were obtained from the measured elastic-to-inelastic (the resonance $4f^{14}6s6p\ ^1P_1$) intensity ratios and absolute DCS values of the $4f^{14}6s6p\ ^1P_1$ state. The ratios were determined at $\theta = 10^\circ$ for all numbered energies, except at 10 eV where the ratio at $\theta = 20^\circ$ was used due to possible influence of the primary electron beam.

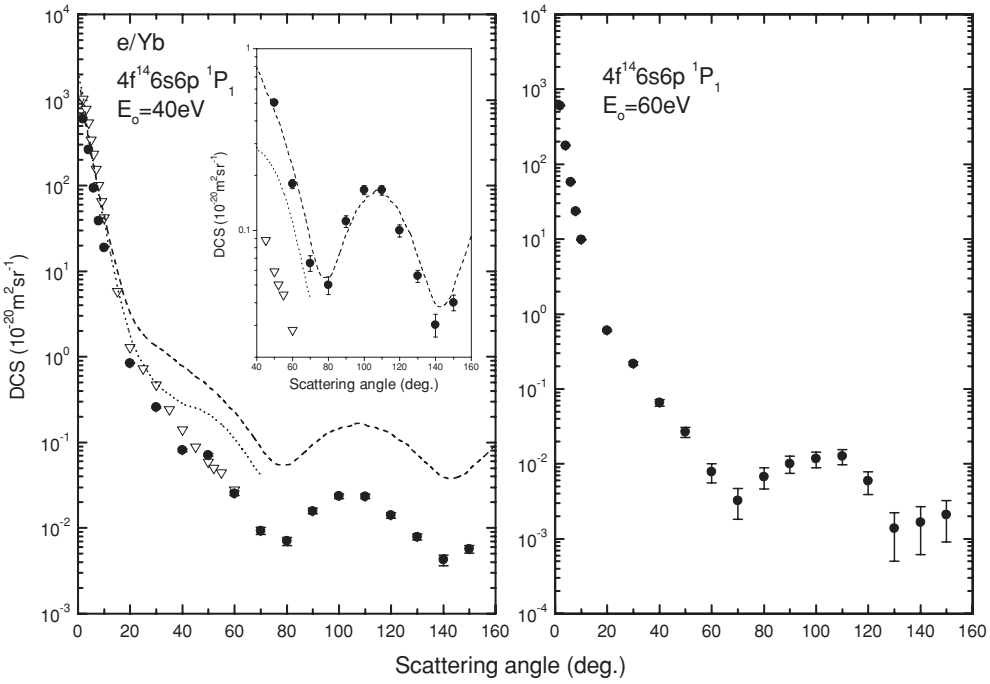

Figure 4. Same as figure 3, but at 40 and 60 eV incident electron energies.

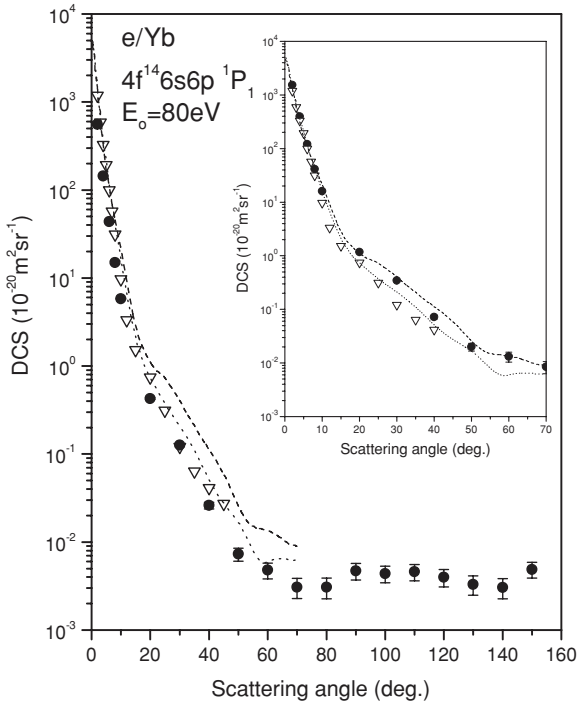

Figure 5. Same as figure 3, but at 80 eV incident electron energy.

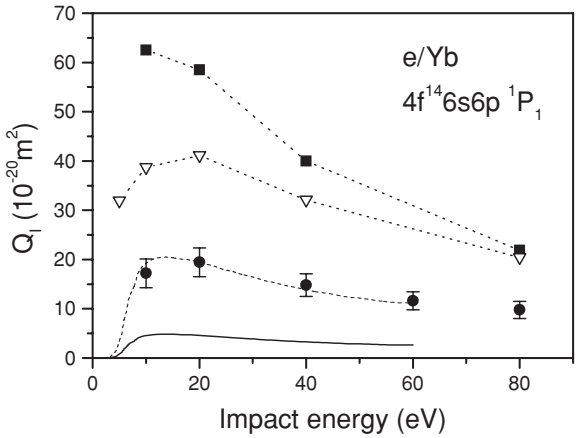

Figure 6. Integral cross sections (Q_I) for electron-impact excitations of the ytterbium atoms ($4f^{14}6s6p\ ^1P_1$ state): Experiments: ●, present (absolute error bars are indicated); —, Shimon *et al* (1981); – – –, Shimon *et al* (1981) normalized to present at 20 eV. Calculations: ▽, UDW Johnson *et al* (1998); ■, RDW Srivastava *et al* (1995). Connecting dotted lines are drawn for ease of viewing.

Table 2. Differential cross sections for elastic electron scattering by ytterbium atoms. The last three rows are integrated—integral (Q_I), momentum transfer (Q_M) and viscosity (Q_V)—cross sections in units of 10^{-20} m^2. The absolute errors are indicated in parentheses.

Scattering angle (°)	DCS (x10^{-20} m^2 sr^{-1})				
	10 eV	20 eV	40 eV	60 eV	80 eV
10	70.5(14.1)	43.8(6.3)	30.3(6.6)	31.0(6.8)	30.2(4.5)
20	9.81(1.97)	6.28(0.90)	5.20(1.13)	7.21(1.58)	6.27(0.95)
30	1.39(0.28)	2.13(0.30)	1.67(0.37)	2.46(0.54)	1.31(0.20)
40	0.988(0.201)	1.70(0.24)	0.827(0.181)	0.852(0.188)	0.297(0.047)
50	0.727(0.148)	1.18(0.17)	0.385(0.084)	0.278(0.062)	0.107(0.018)
60	0.420(0.087)	0.622(0.090)	0.113(0.025)	0.0901(0.0211)	0.0716(0.0130)
70	0.170(0.036)	0.211(0.031)	0.0254(0.0056)	0.0575(0.0139)	0.0643(0.0119)
80	0.114(0.025)	0.0717(0.0110)	0.0306(0.0068)	0.0754(0.0179)	0.0736(0.0130)
90	0.211(0.045)	0.111(0.017)	0.0738(0.0162)	0.0906(0.0212)	0.0533(0.0102)
100	0.339(0.071)	0.208 (0.030)	0.0984(0.0216)	0.0883(0.0207)	0.0578(0.0109)
110	0.285(0.060)	0.278(0.040)	0.0895(0.0196)	0.0625(0.0150)	0.0454(0.0090)
120	0.108(0.024)	0.221(0.032)	0.0613(0.0135)	0.0313(0.0082)	0.0530(0.0102)
130	0.0715(0.0166)	0.170(0.025)	0.0230(0.0051)	0.0106(0.0035)	0.0447(0.0089)
140	0.503(0.103)	0.244(0.036)	0.0968(0.0022)	0.0060(0.0024)	0.0526(0.0101)
150	1.68(0.34)	0.607(0.087)	0.0169(0.0038)	0.0101(0.0034)	0.0974(0.0180)
Q_I	26.6(8.7)	21.5(4.2)	12.2(3.1)	12.2(3.2)	10.5(2.3)
Q_M	8.6(2.8)	4.8(0.9)	1.3(0.3)	1.2(0.3)	1.03(0.23)
Q_V	3.7(1.2)	3.6(0.7)	1.5(0.4)	1.7(0.5)	1.18(0.26)

The absolute DCS values (absolute errors in parentheses) for elastic scattering are presented in table 2. In figure 7 the absolute elastic DCSs with statistical errors are shown. The integrated cross section values together with their total absolute errors are given at the bottom in table 2. These errors arise from the DCS errors, and the extrapolation and numerical integration (0.12).

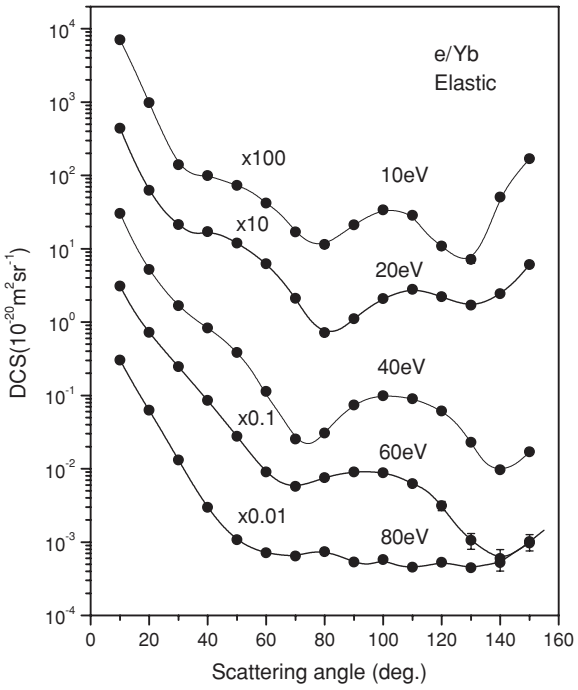

Figure 7. Differential cross sections for elastic electron scattering by ytterbium atoms at 10, 20, 40, 60 and 80 eV impact energies. Statistical error bars are indicated.

4. Discussion and conclusion

The electronic structure of Yb is similar to that of IIb group atoms, used in metal-vapour lasers (Ivanov *et al* 1990), so it was the first of the lanthanides investigated in this direction. In spite of this practical interest, both experimental and calculated data related to elastic and inelastic scattering of electrons by Yb atoms are scarce. For example, angular distributions of elastically scattered electrons by Yb, needed for determination of electron energy distribution functions in the laser medium, is measured for the first time in this work.

A range of E_0 from 10 to 100 eV is classified as a medium energy range where most electron atom interactions must be taken into account. So, the theoretical approach to the electron scattering by ytterbium should be sophisticated, including relativistic effects due to its high Z value.

The energy-loss spectra recorded with energy resolution of 65 meV are good enough to resolve the main inelastic features. Absolute DCS values for the resonance $4f^{14}6s6p\ ^1P_1$ state were of special interest in this work because they served us for putting the relative elastic DCSs to the absolute scale. A linear fit of the GOSs satisfies the FSF for the $4f^{14}6s6p\ ^1P_1$ state in the region determined by OOS for K^2 close to the $K^2_{\min}$. As usual, both the slope of the linear fit decreases and a region of linearity of the GOS shrinks near the $K^2_{\min}$ as E_0 increases. At 10 eV, the data points are linear up to 8°, while at 80 eV only the points at 0°, 2° and 4° lie on the straight line (figure 2).

In comparison with the DCS values measured by Johnson *et al* (1998), the inelastic DCSs obtained in this work are lower by a factor of approximately 2. Also, our results are lower with respect to those obtained by using the RDW approximation (Srivastava *et al* 1995) and

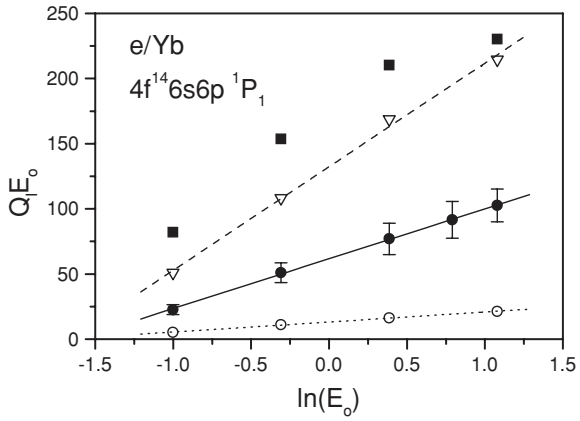

Figure 8. Fano plot for the $4f^{14}6s6p\ ^1P_1$ state of ytterbium. Product of the integral cross sections (Q_I) and incident electron energy (E_0) versus the logarithm of E_0: ●, present (absolute error bars are indicated); ○, Shimon *et al* (1981); ▽, UDW Johnson *et al* (1998); ■, RDW Srivastava *et al* (1995).

UDW approximation (Johnson *et al* 1998). To compare the numbered results in shape, we have renormalized experimental results by Johnson *et al* (1998) to our DCSs at $\theta = 10^\circ$. The agreement is quite good at angles $\theta < 30^\circ$ except at 10 eV impact energy and very low scattering angles (our DCS is more forward peaked, see inset in figure 3). Very good agreement in shape between our and the renormalized experimental DCS by Johnson *et al* (1998) at $E_0 = 20$ eV is presented in the picture inserted in figure 3. At angles $\theta > 30^\circ$ agreement becomes less satisfactory. Extending this kind of analysis to calculations, we have renormalized present DCSs to those of Srivastava *et al* (1995) at $\theta = 110^\circ$ (inset in figure 4) and separately to those of Johnson *et al* (1998) at $\theta = 10^o$ (figure 5). In the first case, the agreement is very good at $\theta \geqslant 50^\circ$ with only available RDW results. In the second case, the agreement is better as the energy increases, at 80 eV much better with RDW than with UDW calculation (see inset in figure 5). Note that at 80 eV impact energy both calculations (UDW and RDW) converge at small scattering angles. There is no DCS available for this state at $E_0 = 60$ eV to compare with.

Present Q_I are lower by a factor of approximately 2 with respect to those calculated by Johnson *et al* (1998) at 80 eV. Present Q_I are in very good agreement with the Shimon results normalized to present at 20 eV, as one can see in figure 6. The RDW calculation by Srivastava *et al* (1995) overestimates Q_I with respect to all numbered experimental and theoretical data.

Comparison of Q_I using the Fano plot method (Fano 1954) is presented in figure 8. Linear functions fit well the data determined experimentally (present, and Shimon *et al* 1981) and theoretically (Johnson *et al* 1998 and Srivastava *et al* 1995 except the point at 80 eV) despite low impact energies where the first Born approximation is unrealistic. Using the equation (Kim and Inokuti 1968)

$$Q_I E_0 = \frac{\pi f_0}{\omega} \ln(4cE_0)$$

where $f_0 \equiv$ OOS and c a constant, we have determined OOS from the slope of the straight line for calculated data by Johnson *et al* (1998). The obtained value of 2.4 disagrees with the experimental value of 1.3 adopted in this work (the values of 1.26 and 1.36 ± 0.06, are given by NIST on line 1999 Data Base and Doidge 1995, respectively). From this fact, the

discrepancy in absolute DCS values between present measurements and those obtained by Johnson *et al* (1998) is understood. The slope of the line obtained from Shimon's results is lower by a factor of approximately 5 with respect to the present. Differences between UDW and RDW have been discussed by Johnson *et al* (1998).

The quotient Q_I/Q_M of the $4f^{14}6s6p\ ^1P_1$ state is a linear function of the incident electron energy in the interval considered. Its slope is larger than in the case of IIb group atoms as a consequence of increasing with energy the low angle with respect to high angle scattering. It means the domination of long range with respect to short range interactions when the energy increases is a remarkable characteristic of the resonance Yb excitation.

The elastic DCSs are forward peaked. If the energy decreases from 80 to 10 eV, general resemblance of the DCSs to $[P_2(\cos\theta)]^2$ is clear. At 80 eV its shape for $\theta > 60^\circ$ is rather flat, but the structure is more marked as the energy decreases: two local minima are more pronounced and an inflection point appears close to $\theta = 30^\circ$. There are no data available to compare with our elastic DCSs. In the energy range considered, the integral cross section for elastic scattering monotonically decreases as electron energy increases. Integral cross sections obtained here are in agreement with the values calculated by Kelemen *et al* (1995).

We can conclude that, in this paper, DCSs for inelastic ($4f^{14}6s6p\ ^1P_1$) and elastic electron scattering by ytterbium are reported in a broad range of scattering angles (to 150°), the elastic for the first time. To the best of our knowledge, the integrated cross sections on the base of experimentally obtained DCSs are determined only in this work. DCSs for the $4f^{14}6s6p\ ^1P_1$ state and elastic electron scattering by ytterbium at 10, 20, 40, 60 and 80 eV incident electron energies could be of interest in the development of high power Yb-vapour lasers. If ytterbium contributes to spectra of an extra terrestrial radiation source (its logarithmic abundance normalized to 10^{12} hydrogen particles per unit volume in the chemical composition of the Sun photosphere is 1.08 ± 0.15, according to table 4.2 in Stix (2002)), the spectra and cross sections reported in this work could be employed in the determination of physical parameters of the astrophysical plasma.

Acknowledgment

This work has been partly supported by MNZZS—Republic of Serbia within the project OI 1424.

References

Avdonina N B, Felfli Z and Murnane A 1997 *J. Phys. B: At. Mol. Opt. Phys.* **30** 2591
Brinkman R T and Trajmar S 1981 *J. Phys. E: Sci. Instrum.* **14** 245
Cahuzac P 1968 *Phys. Lett. A* **27** 473
Chutjian A 1979 *Rev. Sci. Instrum.* **14** 245
Doidge P S 1995 *Spectrochim. Acta* B **50** 209
Fano U 1954 *Phys. Rev.* **95** 1198
Ivanov I G, Latush E L and Sem M F 1990 *Metal Vapour Ion Lasers* (Moskow: Energoatomizdat) and references therein (in Russian)
Johnson P V, Li Y, Zetner P W, Csanak G, Clark R E and Abdallah J 1998 *J. Phys. B: At. Mol. Opt. Phys.* **31** 3027
Kazakov S M and Hristoforov O V 1983 *Opt. Spektrosk.* **54** 750
Keleman V I, Remeta E Yu and Sabad E P 1995 *J. Phys. B: At. Mol. Opt. Phys.* **28** 1527
Kim Y and Inokuti M 1968 *Phys. Rev.* **175** 176
Klimkin V G 1975 *Sov. J. Quantum Electron.* **5** 326
Komarovskii V A 1991 *Opt. Spectrosc.* **71** 322

Mandy J A, Romanyuk M I, Papp F F and Shpenik O B 1993 *Proc. 18th Int. Conf. on the Physics of Electronic and Atomic Collisions (Aarhus)* ed T Andersen, B Fastrup, F Folkmann and H Knudsen (Bristol: Hilger) p 167 Abstracts

Marinković B, Pejčev V, Filipović D and Vušković L 1991 *J. Phys. B: At. Mol. Opt. Phys.* **24** 1817

Milisavljević S, Šević D, Pejčev V, Filipović D M and Marinković B P 2004 *J. Phys. B: At. Mol. Opt. Phys.* **37** 3571

NIST on line 1999 Atomic Spectra Database of the Physics Laboratory of the National Institute of the Standards and Technology, USA

Panajotović R, Pejčev V, Konstantinović M, Filipović D, Bočvarski V and Marinković B 1993 *J. Phys. B: At. Mol. Opt. Phys.* **26** 1005

Panajotović R, Šević D, Pejčev V, Filipović D M and Marinković B P 2004 *Int. J. Mass Spectrom.* **233** 253

Predojević B, Šević D, Pejčev V, Marinković B P and Filipović D M 2003 *J. Phys. B: At. Mol. Opt. Phys.* **36** 2371

Shimon L L, Golovchak N V, Garga I I and Kurta I V 1981 *Opt. Spektrosk.* **50** 1037

Srivastava R, McEachran R P and Stauffer A D 1995 *J. Phys. B: At. Mol. Opt. Phys.* **28** 885

Stix M 2002 *The Sun, An Introduction* 2nd edn (Berlin: Springer)

Takasu Y, Honda K, Komori K, Kumakura M, Takahashi Y and Yabuzaki T 2003 *Phys. Rev. Lett.* **90** 023003